

# Case study: calculation of a narrow resonance with the LIT method

Winfried Leidemann<sup>1,2</sup>

<sup>1</sup>*Dipartimento di Fisica,*

*Università di Trento,*

*I-38100 Trento, Italy*

<sup>2</sup>*Istituto Nazionale di Fisica Nucleare,*

*Gruppo Collegato di Trento, Italy*

(Dated: October 29, 2018)

## Abstract

The possibility to resolve narrow structures in reaction cross sections in calculations with the Lorentz integral transform (LIT) method is studied. To this end we consider a fictitious two-nucleon problem with a low-lying and narrow resonance in the  $^3P_1$  nucleon-nucleon partial wave and calculate the corresponding “deuteron photoabsorption cross section”. In the LIT method the use of continuum wave functions is avoided and one works instead with a localized function  $\tilde{\Psi}$ . In this case study it is investigated how far into the asymptotic region  $\tilde{\Psi}$  has to be determined in order to obtain a precise resolution of the artificially introduced E1 resonance. Comparing with the results of a conventional calculation with explicit neutron-proton continuum wave functions it is shown that the LIT approach leads to an excellent reproduction of the cross section in the resonance region and of further finer cross section details at higher energies. To this end, however, for  $\tilde{\Psi}$  one has to take into account two-nucleon distances up to at least 30 fm.

## I. INTRODUCTION

The LIT approach [1] allows the ab initio calculation of reaction cross sections, where a many-body continuum is involved. The great advantage of the LIT method lies in the fact that the knowledge of the generally complicated many-body continuum wave function is not required. In fact the scattering problem is reduced to a calculation of a localized function with an asymptotic boundary condition similar to a bound-state wave function. The LIT method has been applied to various electroweak cross sections in the nuclear mass range from  $A=3$  to  $A=7$ . Among the applications are the first realistic ab initio calculations of the nuclear three- and four-body total photoabsorption cross sections [2, 3] as well as of the inelastic neutral current neutrino scattering off  $^4\text{He}$  [4]. In addition first ab initio calculations were performed for the total photoabsorption cross sections of  $^4\text{He}$  and  $^6,7\text{Li}$  with semirealistic forces [5, 6, 7]. Other applications were carried out for the inelastic inclusive electron scattering cross section (see e.g. [8, 9, 10]). Further applications and a detailed description of the LIT method are presented in a recent review article [11].

In the past the LIT technique was mainly applied to cases where one has typically rather broad structures (quasielastic peak, giant dipole resonance). One may ask what is the power of the method in presence of narrow resonances in the continuum. In a recent LIT calculation of the  $(e,e')$  longitudinal and transverse form factors of  $^4\text{He}$  [12] a resonance in the Coulomb monopole transition was observed but the width of the resonance could not be determined. Therefore in the present paper we want to address this problem and investigate how narrow resonances can be calculated with the LIT method. To this end we consider a fictitious two-nucleon problem with a low-lying and narrow resonance in the  $^3P_1$  nucleon-nucleon partial wave and calculate the corresponding “deuteron photoabsorption cross section”, which exhibits a pronounced E1 resonance at a photon energy of 2.65 MeV with a width of 270 KeV.

The paper is organized as follows. In sect. II we give a short outline of the LIT calculation of the deuteron photodisintegration. In addition we discuss some aspects of the asymptotic behavior of the LIT solution  $\tilde{\Psi}$ . In sect. III we describe the model for our fictitious NN interaction and show results for the corresponding  $^3P_1$  phase shifts and the photoabsorption cross section calculated in the conventional way with a  $^3P_1$  scattering wave function. The LIT results of our case study are discussed in sect. IV.

## II. THE FORMALISM

The deuteron total photoabsorption cross section is given by

$$\sigma_{\gamma}^d(\omega) = 4\pi^2\alpha\omega R^d(\omega), \quad (1)$$

where  $\alpha$  is the fine structure constant,  $\omega$  is the energy of the photon absorbed by the deuteron, and  $R^d(\omega)$  denotes the response function defined as

$$R^d(\omega) = \sum_f |\langle f|\Theta|0\rangle|^2 \delta(\omega - E_{np} - E_d). \quad (2)$$

Here  $E_d$  and  $|0\rangle$  are the deuteron bound state energy and wave function,  $E_{np}$  and  $|f\rangle$  denote relative kinetic energy and wave function of the outgoing  $np$  pair for a given two-nucleon Hamiltonian  $H$ , and  $\Theta$  is the operator inducing the reaction (it is assumed that recoil effects are negligible). Here we consider the total photoabsorption cross section in unretarded dipole approximation, i.e.

$$\Theta = \sum_{i=1}^2 z_i \tau_i^3, \quad (3)$$

where  $z_i$  and  $\tau_i^3$  are the third components of position and isospin coordinates of the  $i$ -th nucleon.

For a conventional evaluation of  $R^d(\omega)$  one determines the  $np$  scattering wave functions for the induced NN partial waves ( ${}^3P_0$ ,  ${}^3P_1$ ,  ${}^3P_2 - {}^3F_2$ ) and calculates the transitions matrix elements appearing in (2). It is evident that for each of the three partial waves a separate cross section contribution can be defined.

As already mentioned, with the LIT method one avoids the explicit calculation of scattering wave functions. Here one proceeds in the following way. One first calculates the ground state wave function of the nucleus in question, in our case the deuteron. Then one has to solve the equation

$$(H + E_d - \sigma_R - i\sigma_I)|\tilde{\Psi}\rangle = \Theta|0\rangle. \quad (4)$$

Since  $|\tilde{\Psi}\rangle$  is localized one needs to apply only a bound-state technique for the solution of (4). It is convenient to perform multipole decompositions of left- and right-hand sides of (4). In the here considered deuteron case this leads to three separate equations, each one for a different  $\tilde{\Psi}_i$  ( $i=1,2,3$ ). They correspond to the above mentioned three separate  $R^d$  contributions due to the  ${}^3P_0$ ,  ${}^3P_1$ , and  ${}^3P_2 - {}^3F_2$   $np$  final states. The calculation is carried

out for many values of  $\sigma_R$  and a fixed  $\sigma_I$ . A theorem based on the closure property of the eigenstates of  $H$  shows that the sum of the overlaps  $\langle \tilde{\Psi}_i | \tilde{\Psi}_i \rangle$  of the three different multipole solutions of (4) corresponds to the Lorentz integral transform of  $R^d$ ,

$$L^d(\sigma_R, \sigma_I) = \sum_{i=1}^3 \langle \tilde{\Psi} | \tilde{\Psi} \rangle = \int R^d(\omega) \mathcal{L}(\omega, \sigma_R, \sigma_I) d\omega, \quad (5)$$

where  $\mathcal{L}$  is a Lorentzian centered at  $\sigma_R$  and with a width  $\Gamma = 2\sigma_I$ :

$$\mathcal{L}(\omega, \sigma_R, \sigma_I) = \frac{1}{(\omega - \sigma_R)^2 + \sigma_I^2}. \quad (6)$$

The parameters  $\sigma_{R/I}$ , for which (4) is solved, are chosen in relation to the physical problem. In fact  $\sigma_I$  represents a kind of energy resolution for the response function, while the values of  $\sigma_R$  scan the region of interest.

In a final step the transform (5) is inverted in order to obtain the response function and thus the cross section. In the following we use the standard LIT inversion method (alternative inversion methods can be found in [13]), however, with an extension that allows to take care of narrow resonances in the response function.

The standard LIT inversion method consists in the following ansatz for the response function  $R^d$ :

$$R^d(E_{np}) = \sum_{m=1}^{M_{\max}} c_m \chi_m(E_{np}, \alpha_i), \quad (7)$$

where we have replaced the argument  $\omega$  of  $R^d$  by  $E_{np} = \omega - E_d$ . The  $\chi_m$  are given functions with nonlinear parameters  $\alpha_i$ . Here we take

$$\chi_1(E_{np}, \alpha_i) = \frac{1}{(E_{np} - E_{\text{res}})^2 + (\frac{\Gamma}{2})^2} \left( \frac{1}{1 + \exp(-1)} - \frac{1}{1 + \exp((E_{np} - \alpha_3)/\alpha_3)} \right), \quad (8)$$

$$\chi_m(E_{np}, \alpha_i) = E_{np}^{\alpha_4} \exp\left(-\frac{\alpha_5 E_{np}}{m-1}\right) \quad \text{for } m > 1, \quad (9)$$

where in (8) we have set  $E_{\text{res}} \equiv \alpha_1$  and  $\Gamma \equiv \alpha_2$ . It is evident that  $\chi_1$  represents a resonance of Lorentzian shape, where the additional factor in brackets ensures that  $R^d(E_{np})$  is zero for  $E_{np} = 0$ . For  $m > 1$  the set  $\chi_m$  represents the usual basis function set for LIT inversions. Substituting such an expansion into the right hand side of (5) one obtains

$$L(\sigma_R, \sigma_I) = \sum_{m=1}^{M_{\max}} c_m \tilde{\chi}_m(\sigma_R, \sigma_I, \alpha_i), \quad (10)$$

where

$$\tilde{\chi}_m(\sigma_R, \sigma_I, \alpha_i) = \int_0^\infty dE_{np} \frac{\chi_m(E_{np}, \alpha_i)}{(E_{np} - \sigma_R)^2 + \sigma_I^2} . \quad (11)$$

For given values of  $\alpha_i$  and  $M_{\max}$  the linear parameters  $c_m$  are determined from a best fit of  $L^d(\sigma_R, \sigma_I)$  of (10) to the calculated  $L^d(\sigma_R, \sigma_I)$  of (5) for a fixed  $\sigma_I$  and a number of  $\sigma_R$  points much larger than  $M_{\max}$ . In addition one should vary the various nonlinear parameter  $\alpha_i$  over a sufficiently large range. The parameter  $\alpha_4$ , however, can in general be determined from the known threshold behavior of the response function. In fact for our deuteron case one has transitions to  $P$ -waves of the final state and thus  $\alpha_4 = 3/2$ . One starts the inversion by choosing a relatively low value of  $M_{\max}$ , e.g.  $M_{\max} = 6$ , then one selects the overall best fit and repeats the procedure for increasing  $M_{\max}$  up to the point that a stability of the inverted response is obtained and taken as inversion result.

As pointed out above the key point of the LIT approach is the fact that one only works with a function,  $\tilde{\Psi}$ , of finite norm. This localized function  $\tilde{\Psi}$  contains that information of the scattering process which is necessary to calculate reaction cross sections. The asymptotic behavior of  $\tilde{\Psi}$  is described by an exponential fall-off with the argument  $((2m/\hbar^2)\sigma_I)^{1/2}$ , where  $m$  is the nucleon mass and  $\sigma_I$  a parameter of the LIT method, which governs the resolution. The smaller  $\sigma_I$  the better is the resolution and the more extended becomes  $\tilde{\Psi}$ . In other words if one wants to resolve finer structures in the cross section one has to ensure that  $\sigma_I$  is small enough and that  $\tilde{\Psi}$  is calculated sufficiently far enough in the asymptotic region.

In particular, in the following, we investigate up to which two-nucleon distance the localized function  $\tilde{\Psi}$  has to be determined in order to obtain reliable results for the resonance cross section. In addition we also try to simulate the conditions of a LIT calculation for nuclei with more than two nucleons, where usually expansions on complete sets, e.g. hyperspherical harmonic functions, are used. In these cases the solutions  $\tilde{\Psi}$  are obtained in a kind of a spherical box of variable radius  $R_{\max}$ . Beyond  $R_{\max}$   $\tilde{\Psi}$  falls off rapidly. In order to simulate a similar situation, in our case study we use an asymptotic boundary condition for  $\tilde{\Psi}$  leading to a strong fall-off of  $\tilde{\Psi}$  at a two-nucleon distance of  $R_{\max}$  and study the dependence of the results on  $R_{\max}$ .

### III. THE POTENTIAL MODEL

In the following we will use the AV18 NN interaction [14], but modify the  $^3P_1$  potential in order to introduce a fictitious resonance. This is achieved by adding an attractive potential term, i.e.  $V(^3P_1) \rightarrow V(^3P_1) + V_{\text{add}}$ . We take

$$V_{\text{add}} = -\frac{57.6\text{MeV}}{r} (1 - \exp(-2r^2)) \left(1 + \exp\left(\frac{r-5}{0.2}\right)\right)^{-1} \quad (12)$$

with the relative coordinate  $r$  in units of fm.

In Fig. 1 we show the phase shift and in Fig. 2 the “deuteron photoabsorption cross section”  $\sigma_\gamma^d(^3P_1)$  for the modified  $^3P_1$  potential calculated with an explicit  $^3P_1$  continuum wave function. The phase shift exhibits two resonances, one at  $E_{np}=0.48$  MeV and a second one at about 10.5 MeV. For  $\sigma_\gamma^d(^3P_1)$  one finds a very pronounced and narrow resonance at  $\omega=2.65$  MeV with a width  $\Gamma$  of 270 KeV, while the second resonance is about four orders of magnitude weaker and has a width of about 5 MeV. There is a third cross section peak for  $\sigma_\gamma^d(^3P_1)$  at 60 MeV, about 25 times stronger than the second resonance peak, with a rather large width, which cannot be ascribed to a  $^3P_1$  resonance.

### IV. RESULTS AND DISCUSSION

Before we investigate under which conditions one can reproduce the pronounced resonance of  $\sigma_\gamma^d(^3P_1)$  of Fig. 2 via the LIT method, we first want to make another consideration. The smallest cross section width which has been resolved in previous LIT calculation is about 10 MeV (total photoabsorption cross sections of  $^6\text{He}$  [6] and  $^2\text{H}$  [11, 15]). Thus, in order to better understand what was achieved in such calculations, let us first consider the deuteron case with the unmodified AV18 potential. Since we are particularly interested how far the asymptotic range of  $\tilde{\Psi}$  has to be taken into account we proceed for the solution of (4) as follows. For a given value of  $R_{\text{max}}$  we use a boundary condition that requires a strong fall-off of  $\tilde{\Psi}$  at  $R_{\text{max}}$  and calculate the overlap  $\langle \tilde{\Psi} | \tilde{\Psi} \rangle$  of (5) only in the range from  $r = 0$  to  $r = R_{\text{max}}$  (for more details of such a calculation see [11, 16]). In Fig. 3 we show the convergence of  $L^d(^3P_1)$  with respect to  $R_{\text{max}}$  taking, as for other previous LIT calculation of  $\sigma_\gamma^d$  [11, 15],  $\sigma_I = 10$  MeV. One sees that  $R_{\text{max}}=10$  fm is not sufficient, while  $R_{\text{max}}=15$  fm leads already to a rather good approximation of the final result. Convergence is essentially reached with

$R_{\text{max}}=20$  fm. One may ask whether  $\sigma_I=10$  MeV is sufficiently small to resolve the peak structure of  $\sigma_\gamma^d$  in the inversion. A minimal check can be performed in the following way. Let us assume that the cross section is a  $\delta$ -peak at  $E^{\text{peak}}$  with size  $\sigma^{\text{peak}}$ , i.e.

$$\sigma_\gamma^d(E_{np}) = \sigma^{\text{peak}} \delta(E_{np} - E^{\text{peak}}).$$

The resulting LIT is then given by the Lorentzian function

$$L_\delta^d(E^{\text{peak}}, \sigma_R, \sigma_I) = \sigma^{\text{peak}} \mathcal{L}(E^{\text{peak}}, \sigma_R, \sigma_I).$$

In the right panel of Fig. 3 we show such an  $L_\delta^d$ , taking as  $E^{\text{peak}}$  the peak position of  $L^d(R_{\text{max}} = 30 \text{ fm})$  in the left panel of Fig. 3, in addition we set  $L_\delta^d(E^{\text{peak}}) = L^d(E^{\text{peak}})$ . It is readily seen that  $L^d$  has a considerably larger width than  $L_\delta^d$  and thus should contain sufficient information of the peak structure for a reliable inversion. In fact in [11] it was shown that a LIT calculation of  $L^d$  with  $\sigma_I = 10$  MeV leads precisely to the same cross section as a calculation with explicit  $np$  continuum wave functions.

After these initial considerations we turn to  $\sigma_\gamma^d(^3P_1)$  with the modified  $^3P_1$  potential discussed in the previous section. We calculate  $L^d(^3P_1)$  with various  $\sigma_I$  values, namely  $\sigma_I = 10, 5, 2, 1, 0.5$ , and  $0.1$  MeV. First we discuss the convergence of the LIT with respect to  $R_{\text{max}}$  at low energies. In Figs. 4 and 5 we show the cases with  $\sigma_I = 1$  and  $0.5$  MeV as examples. Different from the case considered in Fig. 3,  $R_{\text{max}}=20$  fm is not sufficient to reach a good convergence. For  $\sigma_I = 1$  MeV one finds that the result for  $R_{\text{max}}=30$  fm differs up to about 1% from the converged LIT showing in addition a somewhat oscillatory behavior. With  $R_{\text{max}}=40$  fm one sees a much smoother curve and deviations are reduced to about 0.5%. Very good convergence is reached with  $R_{\text{max}}=50$  fm with deviations of about 0.1%. A rather similar trend can be observed in Fig. 5 for  $\sigma_I = 0.5$  MeV, but the deviations from the converged result are larger, e.g. for  $R_{\text{max}}=30$  fm one has deviations up to 8%, and the oscillatory behavior becomes more pronounced and is even visible for  $R_{\text{max}}=50$  fm. For larger  $\sigma_I$  values (2, 5, 10 MeV) one finds a similar situation as shown in Figs. 4 and 5, but with increasing  $\sigma_I$  relative deviations become smaller and oscillations tend to vanish. For  $\sigma_I = 0.1$  MeV it is not sufficient to take  $R_{\text{max}}=80$  fm in order to have a converged result. This is illustrated in Fig. 6. One observes a steady decrease of the peak height up to an  $R_{\text{max}}$  of almost 140 fm. In order to obtain a smooth result in the whole peak region one has to further increase  $R_{\text{max}}$  up to 300 fm. It is interesting to observe in Fig. 6 how this

convergence is reached with growing  $R_{\max}$ . For values of 30, 60 and 90 fm two, three, and four separate Lorentzians, respectively, are visible. For even greater  $R_{\max}$  the density of single Lorentzians increases further leading finally to a smooth curve for  $R_{\max}=300$  fm. The general picture looks very similar to LIT results obtained by solving  $\tilde{\Psi}$  via an expansion on a complete basis (see e.g. [11]), there an increase of basis states has a similarly effect on existing oscillations as a growing  $R_{\max}$  in our case.

As next point we want to check which value of  $\sigma_I$  should be sufficient to obtain good inversion results at low energies, i.e. leads to a good description of the pronounced resonance peak in the cross section. For this purpose we perform a similar study as has been illustrated in the right panel of Fig. 3. In Fig. 7 we show the corresponding results for  $L^d$  and  $L_\delta^d$  for the various considered  $\sigma_I$  values. For  $\sigma_I = 10$  MeV both results are essentially identical and for  $\sigma_I = 5$  MeV they are almost identical. A further reduction of  $\sigma_I$  leads to more and more differences between  $L^d$  and  $L_\delta^d$ . Finally, for  $\sigma_I = 0.1$  MeV  $L^d$  has a much larger width than  $L_\delta^d$ . Thus one can be rather sure that a very good inversion result should be obtained for the pronounced low-energy resonance with our lowest  $\sigma_I$  value, while  $\sigma_I=10$  MeV should not be sufficient for a reliable inversion. For the other  $\sigma_I$  values it is not clear beforehand whether they suffice, and in the following this will be investigated in detail.

At first, in Fig. 8 we show the results of a minimal inversion, where in (7) we use  $M_{\max}=1$  and hence allow only for a single resonance in the cross section. It is evident that with decreasing  $\sigma_I$  the resonance peak is steadily reduced and the resonance width steadily increased. In the right panel of Fig. 8 a comparison is made between the  $\sigma_I=0.1$  MeV result and the cross section calculated in the conventional way with a  $^3P_1$   $np$  continuum wave function. One finds an excellent agreement in the peak region. Thus it seems that it is necessary to use (i) large  $R_{\max}$  values of far more than 100 fm and (ii)  $\sigma_I$  values equal or smaller than the resonance width  $\Gamma$ . However, in the further discussion we will illustrate that, fortunately, this is actually not the case.

Before we come to the discussion of more complete inversion results, in Fig. 9 we first show the LIT  $L^d$  at higher energies considering three  $\sigma_I$  and various  $R_{\max}$  values. For  $\sigma=5$  MeV and  $R_{\max}=30$  fm one finds slight oscillations beyond 40 MeV, while a larger  $R_{\max}$  leads to a smooth curve. The picture changes for  $\sigma=1$  MeV, oscillations are present in all the three illustrated cases and start already beyond 20 MeV, it is also seen that the oscillation frequency (amplitude) increases (decreases) with growing  $R_{\max}$ . For  $\sigma=0.1$  MeV we only



show the result with  $R_{\text{max}}=300$  fm. One notes that strong oscillations are present beyond 20 MeV.

As next point we turn to the full inversion of  $L^d$ , i.e. not using as for the results of Fig. 8 a restriction of  $M_{\text{max}}$  to 1, but allowing for higher  $M_{\text{max}}$  values. We first consider  $\sigma_I=1$  MeV and take various  $R_{\text{max}}$  values. With  $R_{\text{max}}=20$  fm we do not obtain reasonable results, since the pronounced low-energy resonance cannot be reproduced, instead the best inversion fits are found for a vanishing width  $\Gamma$  of the resonance, which means that a  $\delta$ -peak is preferred. As illustrated in Fig. 10 the situation changes for  $R_{\text{max}}=30$  fm. For the low-energy region one has a very stable inversion result that starts already with  $M_{\text{max}}=7$  and leads to a very good description of the resonance peak. At higher energies the picture is different. None of the inversions describes the region of the second resonance correctly. At even higher energy inversions are improving with increasing  $M_{\text{max}}$  but without reaching a very good agreement with the conventional calculation. The reason for not reproducing the high-energy cross section more precisely is due to the fact that the low-energy resonance contains almost all the  $E1(^3P_1)$  strength. Even for a high-energy  $\sigma_R$  the by far dominant LIT contribution stems from the low-energy resonance region, so that a precise inversion of the high-energy region requires also a very accurate calculation of the LIT. Similar results as for  $\sigma_I = 1$  MeV are also found for  $\sigma_I = 2$  MeV, while our other  $\sigma_I$  values do not lead to a sufficiently good description of the low-energy resonance if  $R_{\text{max}}$  is taken equal to 30 fm. For  $R_{\text{max}}=50$  fm, also shown in Fig. 10, it does not come as a surprise that the low-energy region is described again in an excellent way. In addition for the higher  $M_{\text{max}}$  values one finds a rather good description of the second resonance region and also the high-energy cross section is sufficiently accurate. In Fig. 11 we show results with  $R_{\text{max}}=80$  fm and  $\sigma_I=0.5, 2$ , and 5 MeV. The smaller two  $\sigma_I$  values lead to excellent descriptions of  $\sigma_\gamma^d(^3P_1)$  in the whole considered energy range, only that with  $\sigma_I=0.5$  MeV the cross section is underestimated beyond 120 MeV, while the  $\sigma_I=5$  MeV result exhibits a to 5% too low resonance peak cross section. We do not show inversion results with  $\sigma_I=0.1$  and 10 MeV. They are rather unstable and show oscillations with rather pronounced unphysical negative cross sections.

We summarize our results as follows. We have performed a case study for a LIT calculation with a pronounced resonance in the cross section. To this end the nucleon-nucleon interaction has been modified in the  $^3P_1$  partial wave to generate a fictitious low-lying resonance in the  $np$  continuum. The resulting “deuteron photoabsorption cross section” has

been calculated in two ways: (i) with an explicit  ${}^3P_1$   $np$  continuum wave function and (ii) via the LIT method, i.e. calculating the Lorentz integral transform with subsequent inversion in order to obtain the cross section. The conventional calculation leads to a cross section with three structures: (i) a very pronounced resonance with width of 270 KeV and a peak position of 0.48 MeV above the deuteron break-up threshold, (ii) a second resonance at 10 MeV above threshold with a width of about 5 MeV, which is four orders of magnitude weaker than the first one, and (iii) a rather broad maximum at a photon energy of about 60 MeV with a 25 times higher peak than the second resonance maximum. For a proper resolution of the dominant cross section structure, the pronounced low-energy resonance, one has to consider rather long-ranged solutions  $\tilde{\Psi}$  of the LIT equation, namely at least up to  $R_{\text{max}} = 30$  fm. The cross section results depend strongly also on the LIT parameter  $\sigma_I$ , which governs the resolution (the smaller  $\sigma_I$  the better the resolution). It turns out that it is advantageous to work with  $\sigma_I = 1$  and 2 MeV, about 4-8 times larger than  $\Gamma$ , in this case  $R_{\text{max}} = 30$  fm is sufficient. Even larger  $\sigma_I$  do not correctly reproduce the resonance cross section ( $\sigma_I = 5$  MeV) or even lead to a  $\delta$ -shape resonance ( $\sigma_I = 10$  MeV). Very small  $\sigma_I$  values also lead to disadvantages, since a larger  $R_{\text{max}}$  is required, e.g. with  $\sigma_I = 0.1$  MeV, even taking  $R_{\text{max}} = 300$  fm the LIT is only poorly converged for energies beyond the first resonance region making inversions completely unreliable. Using the intermediate  $\sigma_I$  values and setting  $R_{\text{max}} = 30$  fm one obtains besides the excellent reproduction of the low-energy resonance also a rather good description of the broad maximum at higher energies, while the second, extremely weak, resonance is not well described. An increase of  $R_{\text{max}}$  to 50 fm leads to a rather good description also of the tiny second resonance cross section, and with  $R_{\text{max}} = 80$  fm there is further improvement so that an excellent agreement with the conventional calculation is achieved in the whole considered energy range if  $\sigma_I$  is chosen between 0.5 to 2 MeV.

One might think that for a good description of the low-energy resonance it could be sufficient to restrict the LIT inversion such that only a single resonance is allowed in the cross section. We have shown that this is actually not the case. Even taking  $R_{\text{max}} = 80$  fm one obtains results which show an overestimation of the peak height and an underestimation of the width, e.g. with  $\sigma_I = 5$  MeV (1 MeV) one obtains a width of 90 KeV (180 KeV) instead of 270 KeV and a peak height which is overestimated by a factor of 2.7 (1.4). In addition the resonance is slightly shifted to higher energies. Only for  $\sigma_I = 0.1$  MeV and

$R_{\text{max}} = 300$  fm one finds a very good result for the resonance region. Fortunately, as pointed out in the previous paragraph, the picture changes if one performs a full LIT inversion, i.e. allows for structure besides the resonance.

We think that these findings about the LIT resolution and the proper consideration of the asymptotic extension of the LIT solution  $\tilde{\Psi}$  are generally important for LIT calculations. In particular for methods where  $\tilde{\Psi}$  is expanded on a complete set it has to be ensured that the solution extends far enough into the asymptotic region if one wants to properly resolve cross section structures with a small width. If this is guaranteed the LIT approach opens the possibility to calculate also narrow cross section resonances with great precision.

- 
- [1] Efros VD, Leidemann W, Orlandini G (1994) Phys Lett B **338**:130
  - [2] Efros VD, Leidemann W, Orlandini G, Tomusiak EL (2000) Phys Lett B **484**:223
  - [3] Gazit D, Bacca S, Barnea N, Leidemann W, Orlandini G (2006) Phys Rev Lett **96**:112301
  - [4] Gazit D, Barnea N (2007) Phys Rev Lett **98**:192501
  - [5] Efros VD, Leidemann W, Orlandini G (1997) Phys Rev Lett **78**:4015; Barnea N, Efros VD, Leidemann W, Orlandini G (2001) Phys Rev C **63**:057002
  - [6] Bacca S, Marchisio M, Barnea N, Leidemann W, Orlandini G (2002) Phys Rev Lett **89**:052502; Bacca S, Barnea N, Leidemann W, Orlandini G (2004) Phys Rev C **69**:057001
  - [7] Bacca S, Arenhövel H, Barnea N, Leidemann W, Orlandini G (2004) Phys Lett B **603**:159
  - [8] Efros VD, Leidemann W, Orlandini G (1997) Phys Rev Lett **78**:432
  - [9] Efros VD, Leidemann W, Orlandini G, Tomusiak EL (2005) Phys Rev C **72**:011002(R)
  - [10] Della Monaca S, Efros VD, Khugaev A, Leidemann W, Orlandini G, Tomusiak EL, Yuan LP (2008) arXiv:0801.2880
  - [11] Efros VD, Leidemann W, Orlandini G, Barnea N (2007) J Phys G **34**:R459
  - [12] Bacca S, Arenhövel H, Barnea N, Leidemann W, Orlandini G (2007) Phys Rev C **76**:014003
  - [13] Andreasi D, Leidemann W, Reiss Ch, Schwamb M (2005) Eur Phys J A **24**:361
  - [14] Wiringa RB, Stoks VGJ, Schiavilla R (1995) Phys Rev C **51**:38
  - [15] Barnea N, Leidemann W, Orlandini G (2006) Phys Rev C **74**:034003.
  - [16] Efros VD, Leidemann W, Orlandini G (1993) Few-Body Syst **14**:151

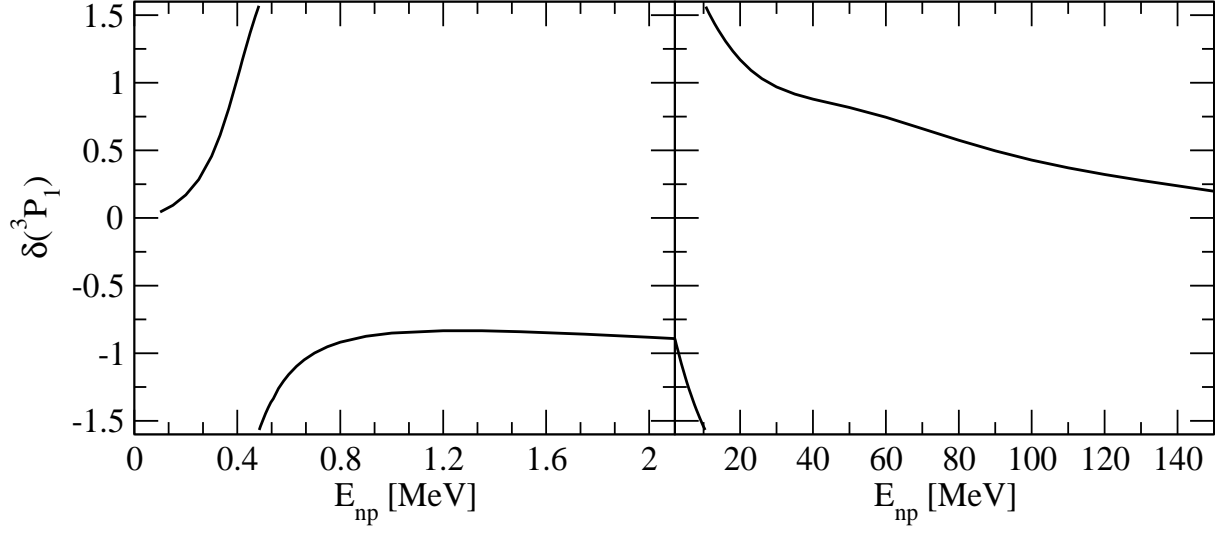


FIG. 1: Phase shift  ${}^3P_1$  with modified  $V({}^3P_1)$  potential at low energy (left) and for extended energy range (right).

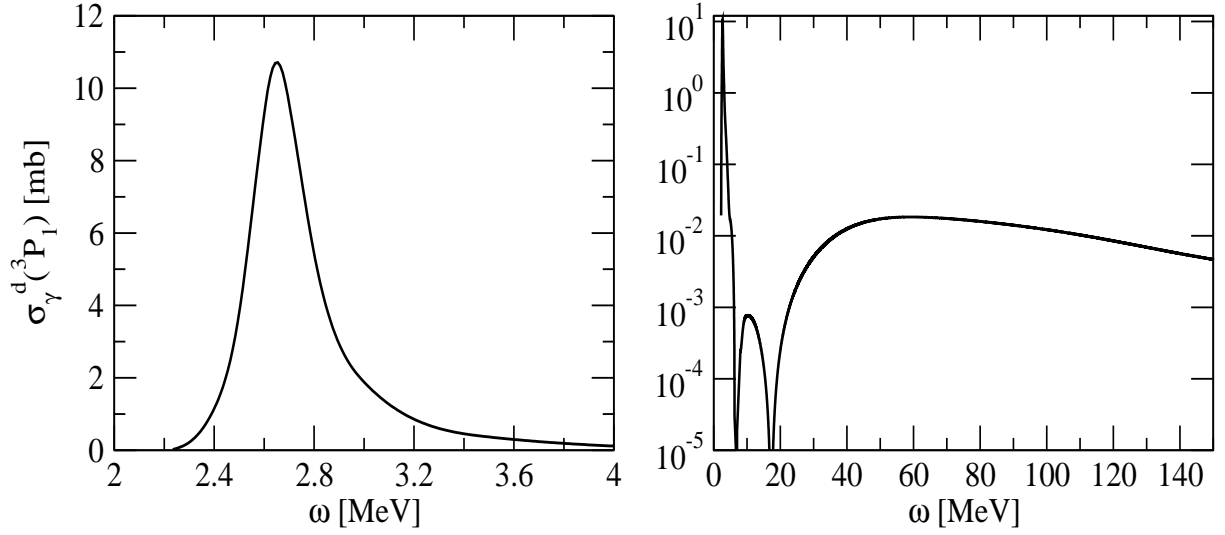


FIG. 2: Photodisintegration cross section  $\sigma_\gamma^d({}^3P_1)$  with modified  $V({}^3P_1)$  potential at low energy (left) and for extended energy range (right).

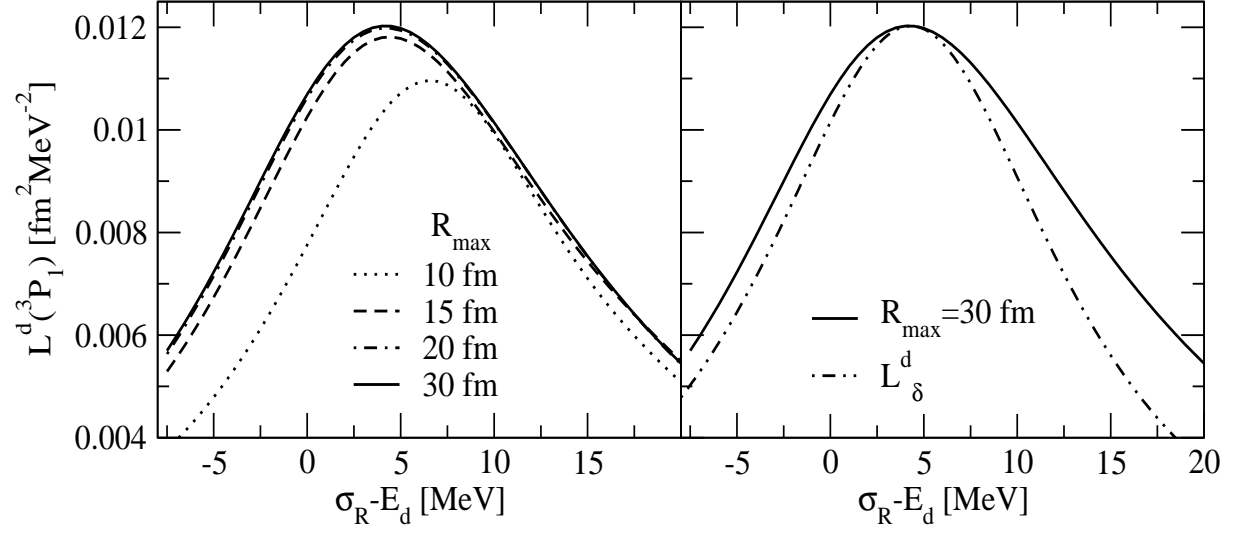


FIG. 3: Lorentz integral transform  $L^d(^3P_1)$  with AV18 NN potential in low-energy region for  $\sigma_I = 10 \text{ MeV}$  and various values of  $R_{\text{max}}$  (left) and comparison of the  $R_{\text{max}} = 30 \text{ fm}$  result with  $L_\delta^d$  (right).

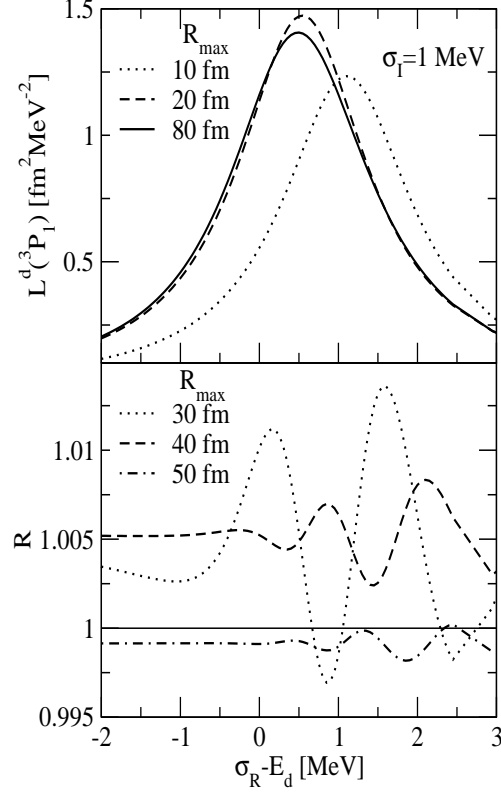


FIG. 4: Lorentz integral transform  $L^d(^3P_1)$  with modified  $V(^3P_1)$  potential in first resonance region for  $\sigma_I = 1 \text{ MeV}$  and various values of  $R_{\text{max}}$  (top) and ratio  $R = L^d(R_{\text{max}}) / L^d(R_{\text{max}} = 80 \text{ fm})$  (bottom).

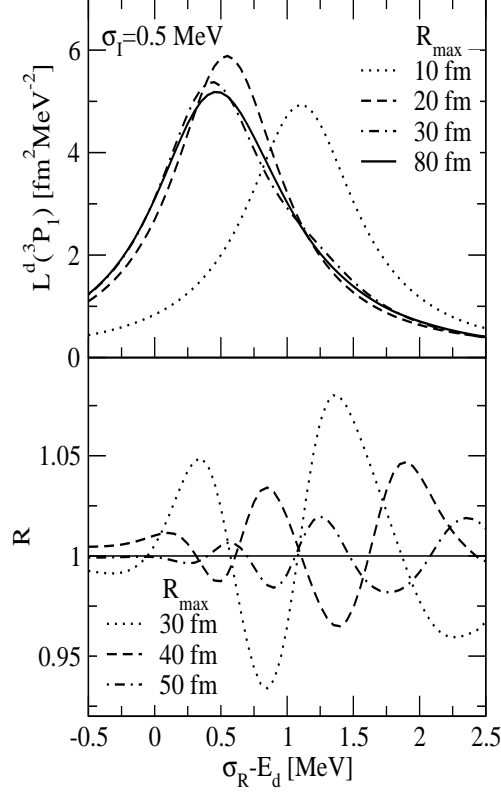


FIG. 5: As Fig. 4 but for  $\sigma_I = 0.5$  MeV

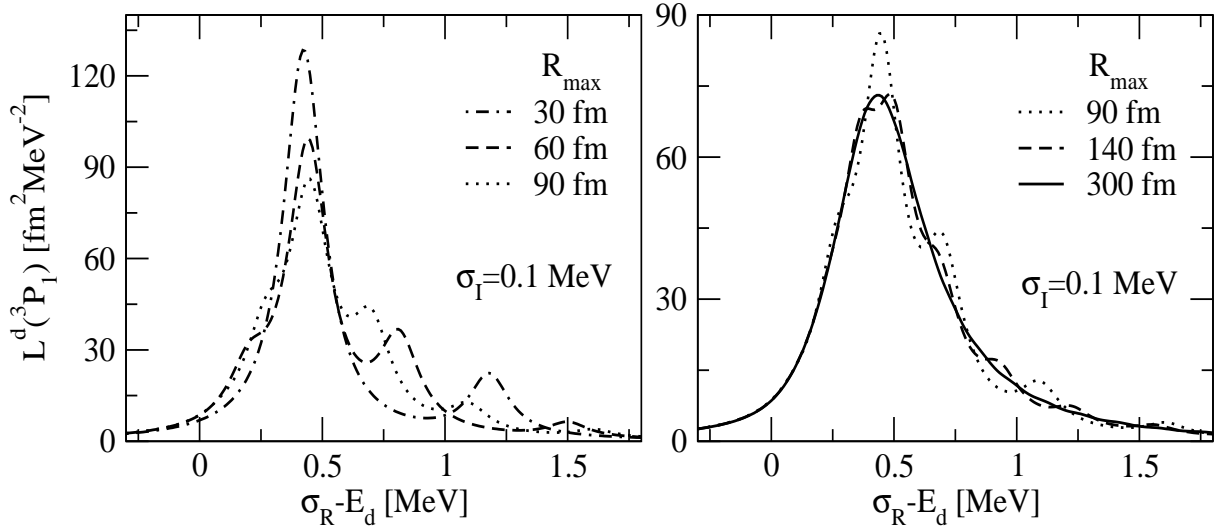


FIG. 6: As Fig. 4 but for  $\sigma_I = 0.1$  MeV and various values of  $R_{\max}$  in both panels.

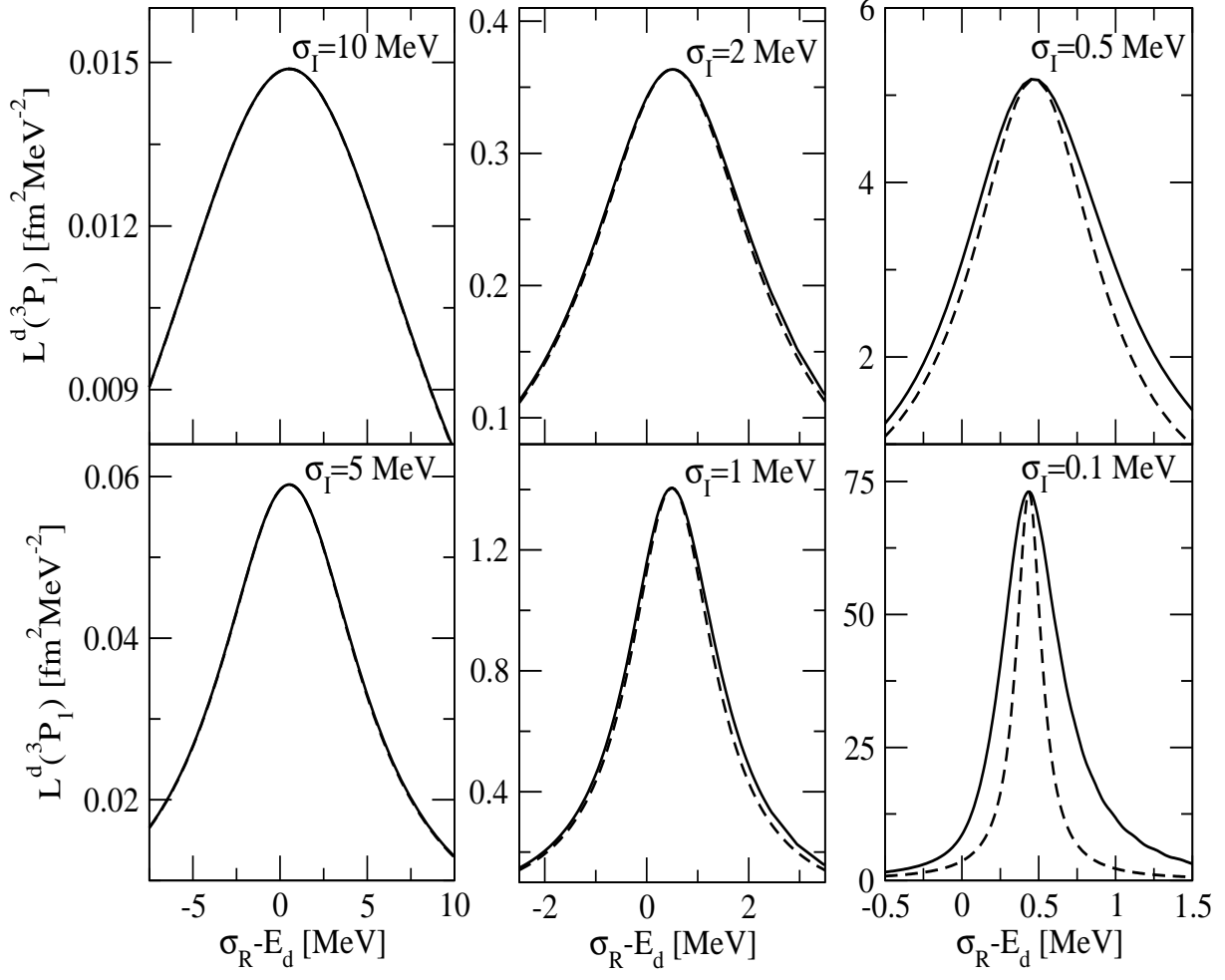


FIG. 7: Lorentz integral transform  $L^d(^3P_1)$  (full curves) with modified  $V(^3P_1)$  potential in first resonance region in comparison to  $L_\delta^d$  (dashed curves) for various values of  $\sigma_I$  with  $R_{\max} = 80$  fm, except for  $\sigma_I = 0.1$  MeV where  $R_{\max}$  is equal to 300 fm.



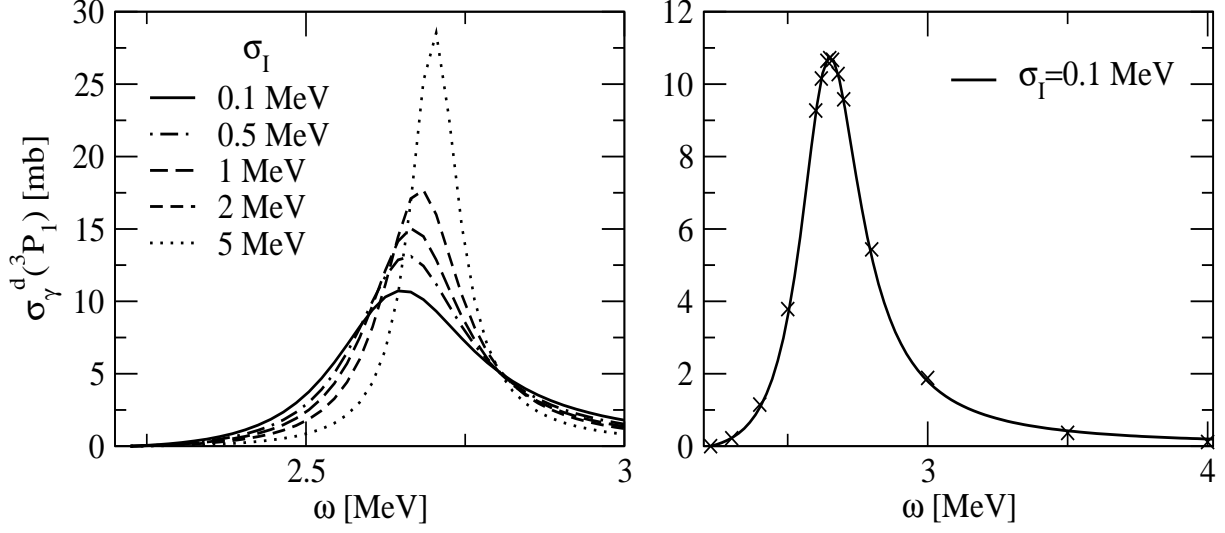


FIG. 8: Cross section  $\sigma_\gamma^d(^3P_1)$  with modified  $V(^3P_1)$  potential in first resonance region obtained from “minimal” inversion with  $M_{\max} = 1$  (see text) for various  $\sigma_I$  values (left) and comparison of the  $\sigma_I = 0.1$  MeV result (full curve) with result of conventional calculation with explicit  $np$  continuum wave functions (crosses).

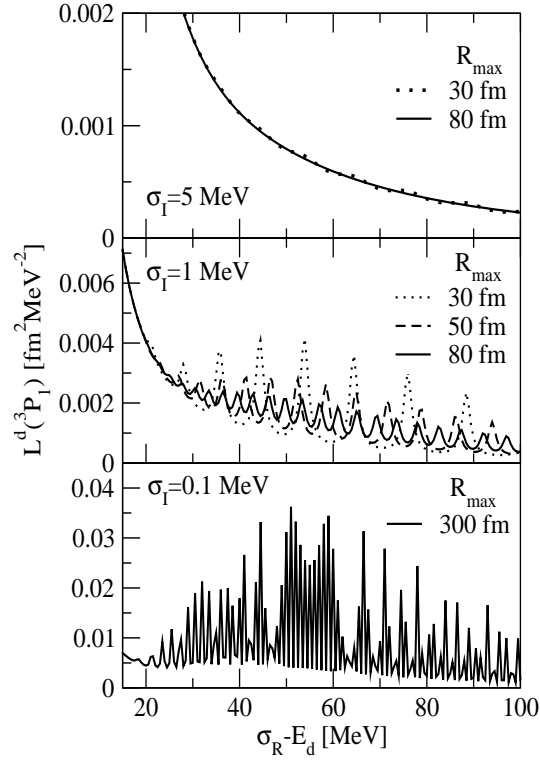


FIG. 9: Lorentz integral transform  $L^d(^3P_1)$  with modified  $V(^3P_1)$  potential beyond first resonance region for  $\sigma_I = 5$  MeV (top), 1 MeV (middle), and 0.1 MeV (bottom) and various values of  $R_{\max}$ .

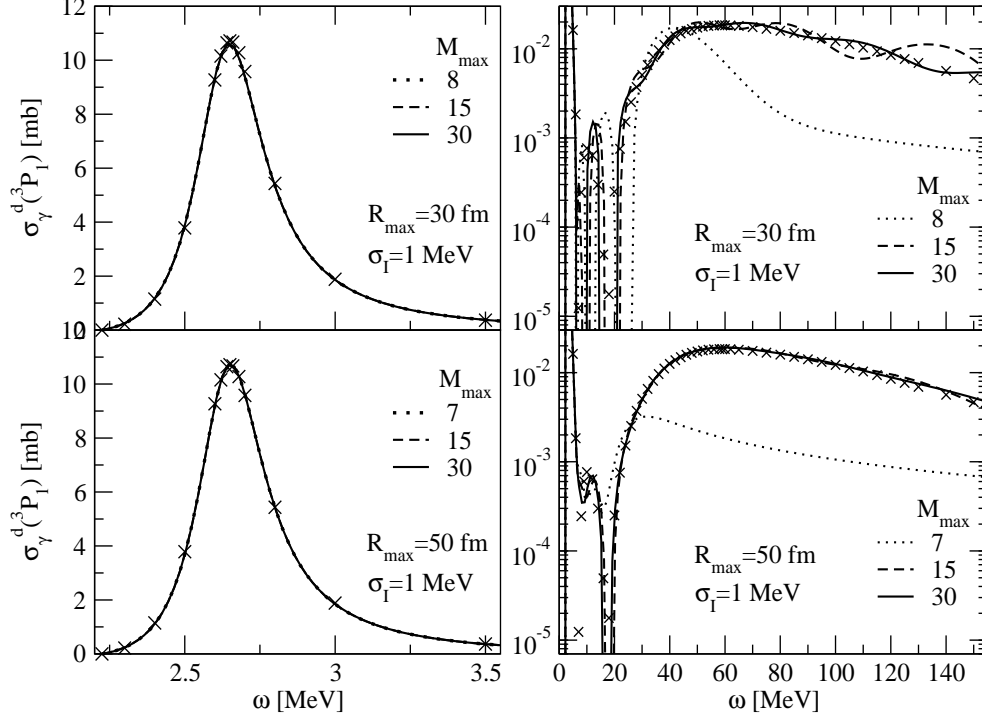


FIG. 10: Cross section  $\sigma_{\gamma}^{d(3P_1)}$  with modified  $V(3P_1)$  potential obtained from inversion of  $L^d(3P_1, \sigma_I = 1 \text{ MeV}, R_{\max})$  with various values of  $M_{\max}$  and for  $R_{\max} = 30$  fm (top) and 50 fm (bottom) in first resonance region (left) and at higher energies (right); also shown results of conventional calculation with explicit  $np$  continuum wave functions (crosses).

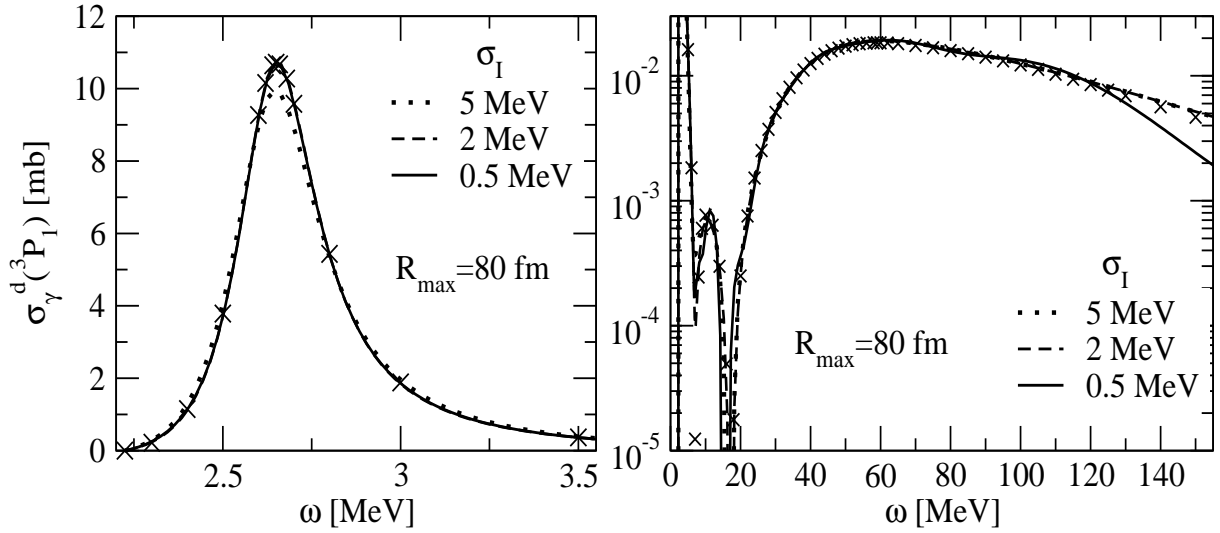


FIG. 11: As Fig. 10 but for  $R_{\max} = 80$  fm and  $\sigma_I = 5, 2$ , and 0.5 MeV.